

## Constraints on Local Segmental Motion in Poly(vinylethylene) Networks

C. M. Roland

Chemistry Division, Code 6120, Naval Research Laboratory, Washington, D.C. 20375-5342

Received March 8, 1994; Revised Manuscript Received May 5, 1994\*

**ABSTRACT:** Dielectric spectroscopy was used to study segmental relaxation in a series of poly(vinylethylene) (PVE) networks. Increasing cross-link density is associated with increasing glass transition temperatures ( $T_g$ ) and broader segmental relaxation functions.  $T_g$ -scaled Arrhenius plots of the segmental relaxation times indicate that enhanced intermolecular coupling is the primary mechanism for the observed changes. This is in contrast to the effects of blending and crystallization, both of which cause changes to the segmental relaxation spectra similar to that from cross-linking. However, the origin of these changes is quite different.

### Introduction

Progress continues to be made in understanding polymer dynamics, with modern theories emphasizing the role of intermolecular constraints on segmental relaxation in dense systems.<sup>1-7</sup> The coupling model of relaxation has played a significant role in these developments,<sup>5-7</sup> in particular because it provides a framework for both predictions and interpretation of the myriad phenomena and anomalies accompanying relaxation in complex fluids. For isolated chains, segmental relaxation involves skeletal bond rotations, with motion over large length scales avoided by cooperative rotations of neighboring units along the chain.<sup>8-11</sup> In dense phase, polymers have their motion further restricted by interaction with nonbonded neighboring segments.<sup>1-7</sup> By introducing into the Hall-Helfand equation<sup>8</sup> describing intramolecular cooperative relaxation of isolated chains a factor to account for the retarding effect of intermolecular constraint, the Kohlrausch-William-Watts function can be obtained,<sup>6</sup> which for the dielectric relaxation function is written

$$\epsilon(t) \sim \exp[-(t/\tau^*)^{1-n}] \quad (1)$$

The coupling parameter ( $0 < n < 1$ ), characterizing the strength of the intermolecular constraints on segmental relaxation, depends on the structure of the relaxing units and on the intermolecular potential. Correlations of chemical structure with  $n$  have been demonstrated for a variety of polymers, as well as small-molecule glass-forming liquids.<sup>12-14</sup> The most useful feature of the coupling model is the relation it provides between the observed relaxation time,  $\tau^*$ , and the intermolecularly uncorrelated relaxation time,  $\tau_0$ .<sup>5-7</sup>

$$\tau^* = ([1 - n]t_c^{-n}\tau_0)^{1/(1-n)} \quad (2)$$

where  $t_c$  is the time after which the intermolecular constraints become manifest.  $\tau_0$ , which can be identified with the intramolecularly correlated Hall-Helfand relaxation time,<sup>8</sup> has a magnitude that depends on the local friction.

Quasielastic neutron scattering experiments, which enable relaxation to be studied over a frequency range extending to very short times, have recently shown<sup>15</sup> that the local segmental motion in poly(vinyl chloride) is in accord with the coupling model. An initially rapid relaxation slows down at a temperature-insensitive time ( $=t_c$ ), after which the stretched exponential form of eq 1

is observed. Molecular simulations also suggest very similar behavior.<sup>16,17</sup>

In addition to the time dependence, the temperature dependence of segmental relaxation is of central importance in understanding the local dynamics of polymers. Because of the weak temperature sensitivity of both  $t_c$  and  $n$ , eq 2 can be rewritten as<sup>18,19</sup>

$$\tau^*(T) \sim \tau_0(T)^{1/(1-n)} \quad (3)$$

Equation 3 illustrates that any temperature dependence of  $\tau_0$ , involving conformational transition rates of isolated chains, will be amplified due to intermolecular cooperativity by the  $1/(1-n)$  power. Consequently, in comparing polymers with similar backbone structures and hence similar  $\tau_0$  temperature dependencies, the observed temperature dependence (i.e., of  $\tau^*$ ) will parallel the magnitude of the coupling parameter. This correlation has been corroborated by a large body of experimental data.<sup>12,13,19-27</sup> If the temperature dependence of the conformational transition rates are the same, the exponent  $1-n$  should scale all measured data to yield a single "universal" relation; that is, the quantity  $(1-n) \log \tau^*$  will exhibit the same temperature dependence for all polymers of similar chemical structure.

Of course, over the range of most experimental measurements, temperature dependencies are non-Arrhenius. Direct comparisons cannot be made, particularly between polymers of very different glass transition temperatures ( $T_g$ ). Some normalization scheme must be employed. Drawing on the ideas of Laughlin and Uhlman,<sup>28</sup> Angell proposed  $T_g$ -normalized Arrhenius plots.<sup>20,21</sup> "Cooperativity curves", that is, semilogarithmic plots of the relaxation time versus  $T_g/T$ , have been used extensively<sup>12-14,19,22,27</sup> and are an established basis for analysis of segmental relaxation data.

Polymers having identical repeat units, but differing in  $T_g$  due to differences in molecular weight, should exhibit segmental relaxations with equivalent degrees of intermolecular coupling. This implies that their cooperativity plots should be equivalent. The demonstration of this for a number of polymers<sup>27,29,30</sup> has directly verified the fundamental connection, implied by eq 3, between the time and temperature dependencies of segmental relaxation.

The assumption underlying eqs 1 and 2 is that the system is comprised of identically relaxing segments, whose motions are correlated. The validity of these relations relies on the absence of any variation among the units themselves or in their relaxation behavior.<sup>31</sup> This assumes

\* Abstract published in *Advance ACS Abstracts*, June 1, 1994.

no intrinsic distribution of relaxation times, as inferred, for example, from free volume models of the glass transition.<sup>32</sup> Criticisms of the latter have been presented.<sup>33–39</sup> If the relaxation is homogeneous, the magnitude of the coupling parameter can be determined directly by fitting data to eq 1. Although any fluctuation in the fundamental relaxation mechanism will obscure the effect of intermolecular coupling on the relaxation function, the correlation of the temperature dependency with the intermolecular coupling strength may still adhere. In this circumstance, cooperativity curves become especially useful for assessing intermolecular cooperativity.

In miscible polymer blends, inhomogeneous broadening due to concentration fluctuations usually dominates the measured relaxation functions. Since segmental relaxation is still governed largely by intermolecular interactions, eqs 2 and 3 provide a means to interpret the observed behavior. Many examples of this approach have been reported.<sup>25,26,29,30,39–41</sup>

A similar situation prevails with semicrystalline polymers. Crystallization broadens the segmental relaxation dispersion, which also shifts to lower frequencies.<sup>42–45</sup> Evidently, amorphous chain segments in proximity to the crystalline phase have their motions restricted by the latter, so that their contribution to the response appears at lower frequencies, thus increasing the measured relaxation time. Nevertheless, it has been shown<sup>46</sup> that the crystalline phase, which does not undergo segmental relaxation, has an insignificant effect on the  $T_g$ -normalized temperature dependence of the segmental relaxation time, at least when the latter is defined in terms of the peak frequency. Thus, temperature dependencies can be used to assess the intermolecular coupling strength in semicrystalline polymers, notwithstanding their inhomogeneously broadened segmental relaxations.

Ostensibly, cross-linking has an effect on segmental relaxation analogous to crystallization. It is well-known that cross-linking increases the glass transition temperature.<sup>47</sup> The precise mechanism for this is not clear. Crystallites can function as physical cross-links,<sup>48</sup> amplifying the mechanical modulus in a qualitatively similar fashion to that of cross-link junctions. A constraint dynamics approach to segmental relaxation has recently been applied to cross-linked rubber.<sup>49</sup> <sup>31</sup>P NMR spin-lattice relaxation measurements on a series of poly-(tetrahydrofuran) networks with tris(4-isocyanatophenyl) thiophosphate junctions<sup>50</sup> were interpreted directly in terms of the intermolecular coupling of the junction dynamics. These NMR results are in agreement with predictions drawn from eqs 1 and 2.<sup>49,50</sup>

The objective of the present work was to distinguish the effect of cross-linking on intermolecular cooperativity from simple increases in local friction (due, for example, to lower free volume or configurational entropy). Poly(vinylethylene) cross-linked with organic peroxide was chosen because segmental relaxation in this polymer is known to be very strongly intermolecularly cooperative<sup>13,41</sup> and because the carbon-carbon junctions in such networks minimally perturb the intermolecular potential, making application of eq 3 more justifiable.

## Experimental Section

The PVE was 96% 1,2-polybutadiene (obtained from the Firestone Tire & Rubber Co.) having number- and weight-average molecular weights equal to 134 000 and 153 000, respectively. Varying quantities of dicumyl peroxide cross-linker (Varox DCP-R from the R.T. Vanderbilt Co.) were added to solutions of the polymer in cyclohexane. Cast films (typically 0.25-mm thick) were dried and then cured 30 min at 423 K (see Table 1).

Table 1. Poly(vinylethylene) Networks

	cross-linker (wt %)	modulus (MPa) <sup>a</sup>	$N^b$	$T_g$ (K) <sup>c</sup>	log $A$	$B$	$T_e$	$n^d$
PVE-0	0	0		272.5	-11.33	747.0	240.1	0.59
PVE-5	0.056	<i>e</i>	<i>e</i>	276.8	-10.77	715.6	245.6	0.61
PVE-11	0.111	1.8	70	279.5	-10.08	912.0	244.6	0.63
PVE-22	0.222	3.8	28	282.7	-11.36	724.6	252.9	0.65
PVE-44	0.444	6.4	21	285.2	-20.18 <sup>f</sup>	2698 <sup>f</sup>	224.8 <sup>f</sup>	0.66
PVE-66	0.666	57	2 <sup>g</sup>	287.7	-8.82	346.1	269.0	0.67

<sup>a</sup> Uniaxial tensile stress divided by elongation at mechanical equilibrium. <sup>b</sup> Number of monomer units per elastically active network chain (eq 4). <sup>c</sup> Taken to be the temperature at which the maximum in the dielectric loss occurs at 1 Hz. <sup>d</sup> For networks, the coupling parameter was estimated scaled from cooperativity plot (Figure 5). <sup>e</sup> Sample integrity was too poor for reliable mechanical measurements. <sup>f</sup> Due to experimental scatter in the  $\tau^*$  data, the fit to eq 5 is not unique. <sup>g</sup> Lower limit (eq 4 not applicable).

Conductivity, which interferes with dielectric constant measurements at lower temperatures, was reduced by extracting the cured rubber in an excess of solvent (sequentially THF and acetone). All experiments were carried out on the extracted networks.

The structure of the networks was characterized by measuring the equilibrium deformation under uniaxial tension. Samples were dead weighted (0.2–1 MPa) and the displacement of fiducial marks recorded 1 day later. In order to ensure that mechanical equilibrium was attained, the stretched rubbers were warmed to ca. 50 °C and then allowed to cool to room temperature prior to measurement of the strain.

Dielectric experiments employed a time domain spectrometer (IMASS Inc.), which is based on the transient current method.<sup>51</sup> The numerically transformed data cover the frequency range from 10<sup>-4</sup> to 10<sup>4</sup> Hz, although dc conduction interferes with the lower frequency results. Since PVE is not very polar, high sensitivity was necessary; for the more cross-linked samples, experiments were carried out at 1–2 pF full scale. The sample cell was a pair of 25-mm aluminum plates with a guard ring on the detector side. Sample films were placed between the spring-loaded plates 1 day prior to measurements in order to ensure good contact. The temperature stability of the sample chamber (Delta Design Model 9023) was better than ±0.05 K. The temperature was monitored at the sample position, although uniformity within the chamber was at least 0.1 K.

## Results and Discussion

Rubber elasticity models allow the equilibrium modulus of cross-linked rubber to be interpreted in terms of the network structure. When PVE is reacted with dicumyl peroxide, the free radical formed at the vinyl carbon rapidly propagates with minimal termination;<sup>52</sup> this yields cross-link junctions of very high functionality. For such junctions the affine limit applies,<sup>53</sup> whereby at equilibrium the true stress is related to the degree of polymerization of the network chains,  $N$ , according to

$$\sigma = \frac{\rho RT}{mN}(\lambda^2 - \lambda^{-1}) \quad (4)$$

In this equation  $\lambda$  is the stretch ratio and the repeat unit molecular weight,  $m$ , equals 54 for PVE. The mass density of the un-cross-linked polymer was used;  $\rho = 0.883$  g/cm<sup>3</sup>. The measured moduli and calculated values of  $N$  are listed in Table 1.

Certainly at the highest cross-link density (PVE-66), the network chains are insufficiently flexible for eq 4 to apply; that is, the assumption of a Gaussian distribution of end to end vectors is violated for very short strands. This is reflected in the modulus measured for PVE-66 (Table 1), which is much larger than that of the other networks and out of proportion to its level of cross-linker. Cross-linking to this high a degree produces a substantial

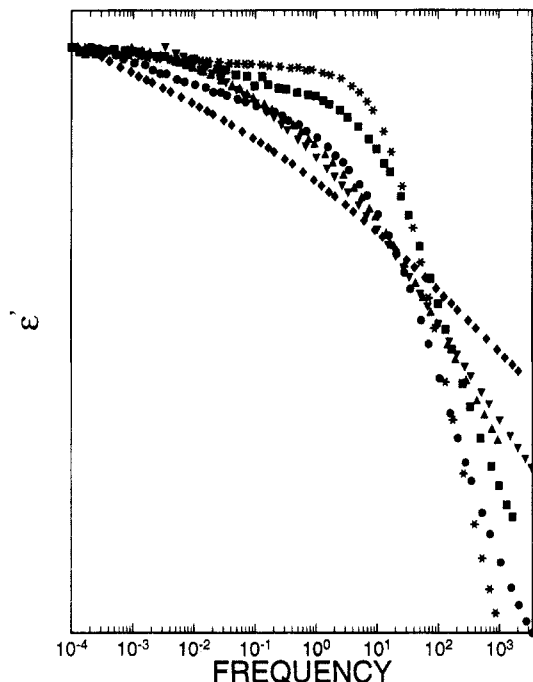


**Figure 1.** Dielectric constant measured for the linear PVE and the five networks. The data, displayed semilogarithmically, have been vertically scaled and horizontally shifted to facilitate comparison of the shapes in the vicinity of the glass transition. In this and the ensuing Figures 2–5, the symbols correspond to (\*) PVE-0, (■) PVE-5, (●) PVE-11, (▲) PVE22, (▼) PVE-44, and (◆) PVE-66.

portion of short network chains, whose contribution to the measured stress will be disproportionately large due to finite extensibility. However, there is no reason to expect that a departure from “Gaussian chain” behavior at higher cross-link density should directly influence the local segmental dynamics. Segmental relaxation primarily involved correlated local motion of only a few backbone bonds,<sup>4,11</sup> whereas a Gaussian distribution of vectors requires chain segments containing on the order of 50 or more atoms.<sup>54</sup> Hence, the discontinuity in the modulus for PVE-66 is not accompanied by any discontinuity in the effect of cross-linking on segmental relaxation behavior.

Representative dielectric constant and loss spectra are shown in Figures 1 and 2, respectively. The transition associated with segmental relaxation systematically broadens with increasing cross-link density. Similar broadening was recently reported for cross-linked styrene-butyl acrylate copolymers.<sup>55</sup> In that study an attempt was made to interpret the shape of the relaxation function directly in terms of various models and empirical equations. We eschew this approach, reflecting the belief that a randomly cross-linked polymer will consist of chain segments exhibiting different dynamics corresponding to their proximity to the network junctions. Segments closer (topologically or spatially) to a junction are expected to have their motions more retarded. This is especially true for junctions of very high functionality like those in peroxide cross-linked PVE, wherein the confluence of many strands at the junction site imposes severe steric constraints.<sup>56</sup> The contribution of such segments to the measured dielectric response appears at lower frequencies, shifting the observed maximum in the dispersion to lower frequency. The inhomogeneously broadened dispersions in cross-linked PVE (Figure 2) no longer exhibit the stretched exponential form (eq 1), whereby assessment of intermolecular coupling strength cannot be accomplished by curve fitting.

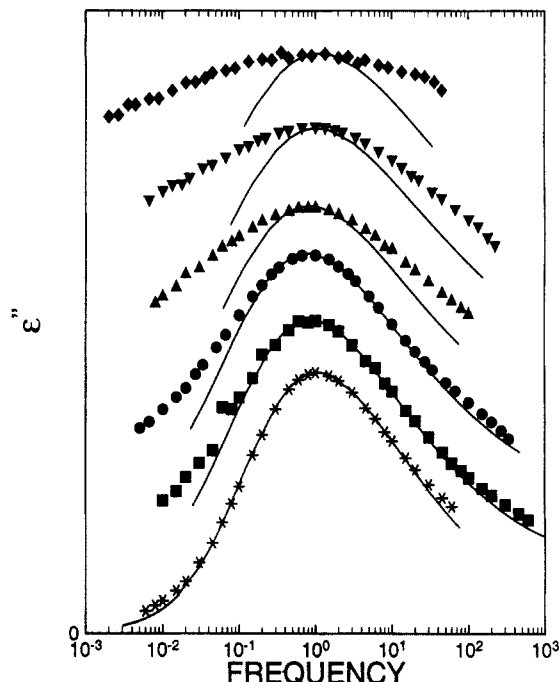


**Figure 2.** Segmental relaxation dispersion in the dielectric loss for linear PVE and the five networks (symbols correspond to those in Figure 1). The peaks have been arbitrarily shifted to illustrate the systematic broadening accompanying increasing cross-link density. The solid lines were calculated using eq 1, with the values of  $n$  determined from superpositioning the cooperativity curves (see Figure 5). The measured experimental dispersions are broader, particularly at the higher cross-link densities, due to inhomogeneous broadening.

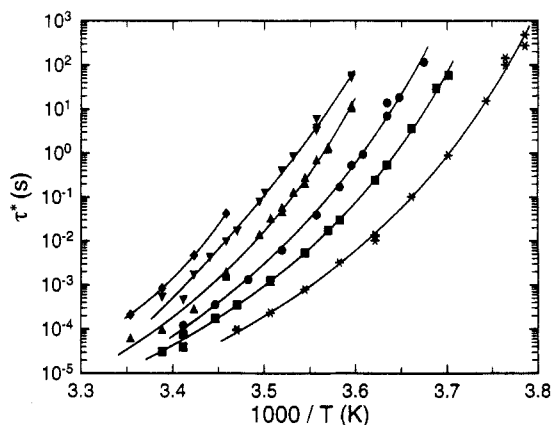


**Figure 3.** Segmental relaxation times, defined from the peak frequencies, for PVE (symbols as defined in Figure 1), with the fits to eq 5 shown as the solid lines. There is a systematic increase in relaxation time and glass transition temperature with increasing cross-link density.

Since we cannot fit the measured relaxation to eq 1, the relaxation time is defined using the peak frequency of the dispersion,  $\tau^* = 1/2\pi f_p$ . The variation of this quantity with temperature is shown in Figure 3 for all networks. The glass transition temperature of the networks is taken to be the temperature at which the peak frequency equals 1 Hz ( $\tau^* = 0.159$  s). To facilitate interpolation between the measurement temperatures, the data in Figure 3 were fitted to the Vogel equation<sup>54</sup>

$$\tau^* = A \exp\left(\frac{B}{T - T_\infty}\right) \quad (5)$$

The results are given in Table 1. The most cross-linked rubber has a glass transition temperature 15 K higher than the linear PVE.

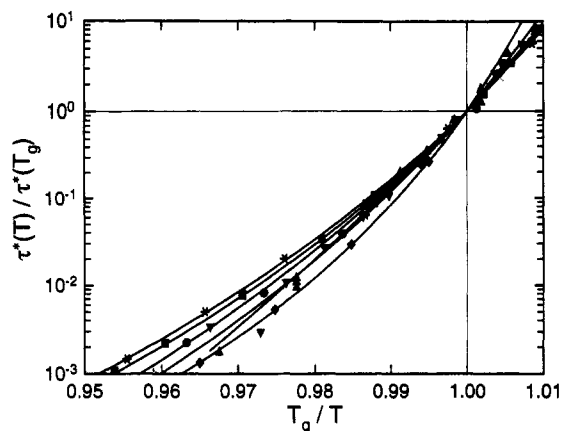


**Figure 4.** Cooperativity plots corresponding to the Arrhenius curves in Figure 3. The steepest curves are those for PVE networks of highest cross-link density.

Using the  $T_g$  values in Table 1, cooperativity plots were constructed (Figure 4). The striking feature therein is the systematic increase in temperature sensitivity with increasing cross-link density. This indicates that segmental relaxation in the more cross-linked networks is associated with stronger intermolecular coupling. This contrasts with the effect of crystallinity on segmental relaxation. When temperatures are normalized by  $T_g$ , the temperature dependence of segmental relaxation times are found to be independent of the degree of crystallinity.<sup>46</sup> The constraints on segments in proximity to crystallites increase their relaxation time; however, the degree of intermolecular coupling for most chain units is unaffected. The shift of the peak frequency, which represents the average chain environment, is altered mainly as a consequence of increased local friction. This affects only  $\tau_0$ , but not  $n$  or the  $T_g$ -normalized temperature dependence.

The stronger intermolecular coupling of the networks indicates that the junctions and the chains emanating from them are effectively constraining local motion of segments well-removed from the junction sites. The question remains whether the increases in  $T_g$  (Table 1) are entirely due to this enhanced intermolecular coupling or whether there is also a contribution from enhanced local friction (i.e., higher  $\tau_0$ ). Equation 2 can be used to address this issue; however, this requires a quantitative measurement of the coupling parameters of the networks.

To obtain values for  $n$ , we make use of eq 3 to attempt a superpositioning of the cooperativity curves in Figure 4. The scaling exponent,  $1 - n$ , required to superpose the data yields a measurement of the coupling parameter for each network. This analysis assumes that  $n$  is independent of temperature, which is not strictly true for PVE. An extensive study using both mechanical and dielectric spectroscopy has been carried out on linear PVE.<sup>57</sup> Although the coupling parameter at a given temperature was equivalent as measured by either spectroscopy,  $n$  did vary by 0.04 over a 15 K temperature range. To the extent cross-linking does not modify this temperature dependence, the interpretation of the cooperativity curves for PVE networks is unaffected. In the present work we find for the linear polymer (PVE-0) that  $n = 0.59$  at temperatures in the vicinity of  $T_g$ ; this is consistent with the earlier study.<sup>57</sup>

Scaled cooperativity plots are shown in Figure 5. The superpositioning of the curves is well within the scatter in the data. (This experimental scatter is more prominent for the networks of higher cross-link density, partly because their dispersions are broader, making determination of the peak frequency more uncertain.) The "best-fit" values

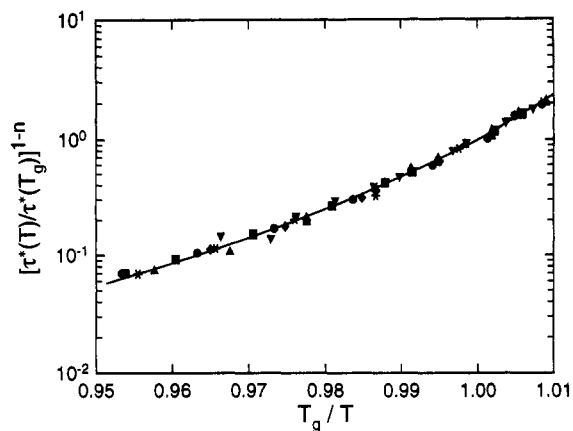


**Figure 5.** Data in Figure 4 with each curve scaled by the exponent  $1 - n$  (see eq 3). The values for the coupling parameters yielding superpositioning of the data are given in Table 1.

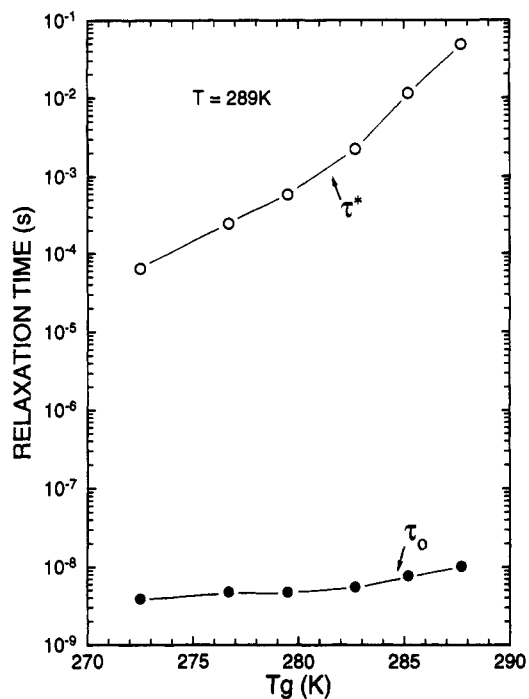


**Figure 6.** Intermolecularly cooperative ( $\tau^*$ ) and noncooperative ( $\tau_0$ ) relaxation times for the PVE, with the samples identified by their measured glass transition temperatures (given in Table 1). The  $\tau_0$ 's were calculated from the respective  $\tau^*$  (measured at  $T = 289$  K) using eq 2 and the value of  $n$  determined from construction of Figure 5.

for the coupling parameters are listed in Table 1. It should be emphasized that using these  $n$ 's in eq 1 yields peaks that are narrower than observed experimentally; this is illustrated in Figure 2. There is significantly more intensity, particularly on the low frequency side, than is given by the stretched exponential function. This divergence of the experimental data reflects inhomogeneous broadening.

Using the values for the coupling parameters deduced from scaling the cooperativity plots (Table 1), we can calculate via eq 2 the value of  $\tau_0$  for each network. The comparison is made at a temperature ( $T = 289$  K) for which extrapolation of the measured data is avoided, with the fitted Vogel parameters (eq 5) used to interpolate the measured  $\tau^*$ . From the results (Figure 6), we conclude that most of the modification of PVE's segmental dynamics results from enhanced intermolecular coupling. There is only a very modest increase in  $\tau_0$  with cross-linking, indicating only a slight alteration of the friction coefficient

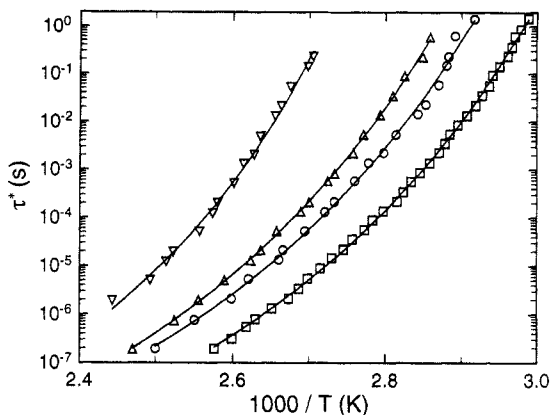


**Figure 7.** Relaxation times taken as the frequency of the peak for styrene-butyl acrylate copolymers (reported in ref 55). Solid lines represent the Vogel fits (eq 5), and the symbols correspond to 0% (□), 5% (○), 10% (Δ), and 20% (▽) divinylbenzene cross-linker in the polymer backbone.

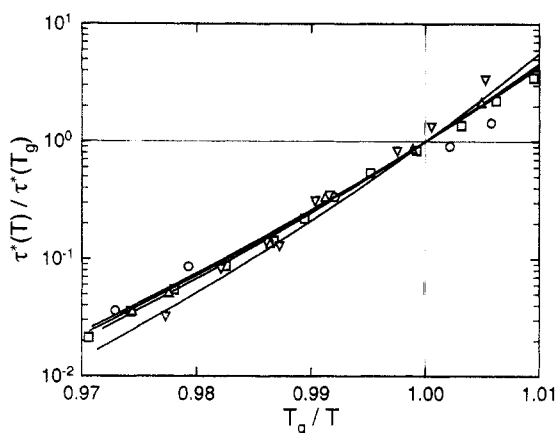


**Figure 8.** Cooperativity plots constructed from the data in Figure 7, with  $T_g$  defined as the temperature at which the peak in the dielectric loss occurs at 10 Hz.

due to cross-linking. Thus, even though cross-linking and crystallization both broaden the segmental relaxation function and elevate the glass transition temperature, different mechanisms are operative.

In Figure 7 we display an Arrhenius plot of segmental relaxation times, the data taken from a recent dielectric study<sup>55</sup> of styrene-butyl acrylate copolymers cross-linked with varying amounts of divinylbenzene. Cross-linking shifts the transition to higher temperatures and also broadens the dispersion in the dielectric loss.<sup>55</sup> We extract from this data a glass transition temperature, taken to be the temperature at which the peak frequency equals 10 Hz. (This is a higher frequency than in the present PVE work because the dielectric experiments of ref 55 were obtained with a higher frequency spectrometer.) Normalizing the data in Figure 7 with this operationally defined  $T_g$ , we obtained cooperativity curves for the four networks (Figure 8). The data are somewhat scattered, but it does appear that at least the most cross-linked network shows a significant increase in  $T_g$ -scaled temperature dependence. Although this system may not be ideal for our purposes (due to the presence of three distinct monomer units of differing polarity in the precursor chains), the results in Figure 8 are not inconsistent with conclusions drawn from the PVE experiments.

## Summary

When there are no fluctuations of the relaxing species, a homogeneous relaxation process, described by eq 1, often

results. Neat, amorphous, linear polymers exemplify this situation. Three circumstances are known to cause broadening of the segmental relaxation function, along with a shift of the relaxation time. In polymer mixtures, nonuniformity of the local environment, due to concentration fluctuations, effects a distribution of relaxation behaviors. Both the strength of the intermolecular coupling and the magnitude of the local friction vary within a blend. In the language of the coupling model, both  $n$  and  $\tau_0$  are distributed. Crystallization also introduces compositional nonuniformity; however, the principal consequence is a change in the average relaxation time without a change in the coupling strength. That is, crystallization primarily affects only  $\tau_0$  and not  $n$ , at least for the majority of segments, which lay distant from the crystallites. Chain segments adjacent to the crystalline phase may experience more severe constraints on their dynamics. However, their contribution to the measured relaxation falls at higher frequencies, whereby cooperativity curves constructed using peak frequencies are unaffected.<sup>46</sup>

A third source of inhomogeneous broadening, cross-linking, was the focus of the present study. The results indicate that intermolecular coupling is enhanced in networks (higher  $n$ ), accompanied by only a slight increase in the noncooperative relaxation time,  $\tau_0$ . The effect of cross-linking on segmental relaxation is thus distinctly different from that of blending or crystallization, at least when considering local segmental dynamics. Currently we are investigating the manner in which heterogeneity of the polymer backbone, for instance, as in random copolymers, modifies segmental relaxation.

**Acknowledgment.** We thank J. J. Fitzgerald of Eastman Kodak Co. for making his data on styrene-butyl acrylate copolymers available prior to publication. Stimulating conversations with K. L. Ngai of NRL and J. P. Runt of The Pennsylvania State University are gratefully acknowledged. This work was supported by the Office of Naval Research.

## References and Notes

- (1) Matsuoka, S. *Relaxation Phenomena in Polymers*; Hanser: Munich, 1992.
- (2) Matsuoka, S.; Quan, X. *Macromolecules* **1991**, *24*, 2770.
- (3) Schonhals, A.; Schlosser, E. *Colloid Polym. Sci.* **1989**, *267*, 125.
- (4) Bahar, I.; Erman, B.; Kremer, F.; Fischer, E. W. *Macromolecules* **1992**, *25*, 816.
- (5) Ngai, K. L.; Rendell, R. W.; Rajagopal, A. K.; Teitler, S. *Ann. N.Y. Acad. Sci.* **1986**, *484*, 150.
- (6) Ngai, K. L.; Rendell, R. W. *J. Non-Cryst. Solids* **1991**, *131-133*, 942.
- (7) Ngai, K. L.; Peng, S. L.; Tsang, K. Y. *Physica A* **1992**, *191*, 523.
- (8) Hall, C. K.; Helfand, E. *J. Chem. Phys.* **1982**, *77*, 3275.
- (9) Dejean de la Batie, R.; Laupretre, F.; Monnerie, L. *Macromolecules* **1988**, *21*, 2045.
- (10) Bahar, I.; Erman, B.; Monnerie, L. *Macromolecules* **1991**, *24*, 3618.
- (11) Adolf, D. B.; Ediger, M. D. *Macromolecules* **1992**, *25*, 1074.
- (12) Roland, C. M.; Ngai, K. L. *Macromolecules* **1991**, *24*, 5315; **1992**, *25*, 1844.
- (13) Roland, C. M. *Macromolecules* **1992**, *25*, 7031.
- (14) Ngai, K. L.; Roland, C. M. *Macromolecules* **1993**, *26*, 6824.
- (15) Colmenero, J.; Alegria, A.; Arbe, A.; Frick, B. *Phys. Rev. Lett.* **1992**, *69*, 478.
- (16) Roe, R.-J.; Rigby, D.; Furuya, H.; Takeuchi, H. *Comput. Polym. Sci.* **1992**, *2*, 32.
- (17) Roe, R.-J. *J. Chem. Phys.* **1994**, *100*, 1610.
- (18) Ngai, K. L.; Rendell, R. W.; Plazek, D. J. *J. Chem. Phys.* **1991**, *94*, 3018.
- (19) Plazek, D. J.; Ngai, K. L. *Macromolecules* **1991**, *24*, 1222.
- (20) Angell, C. A. In *Relaxations in Complex Systems*; Ngai, K. L., Wright, G. B., Eds.; Government Printing Office: Washington, DC, 1985; p 3.

- (21) Angell, C. A. *J. Non-Cryst. Solids* 1991, 131-133, 13.
- (22) Ngai, K. L. *J. Non-Cryst. Solids* 1987, 95-96, 969.
- (23) Torell, L. M.; Grimsditch, M. *Proc. Phys.* 1989, 37, 196.
- (24) Dixon, P.; Wu, L.; Nagel, S.; Williams, B. D.; Carini, J. P. *Phys. Rev. Lett.* 1990, 65, 1108.
- (25) Roland, C. M.; Ngai, K. L. *Macromolecules* 1992, 25, 363.
- (26) Ngai, K. L.; Roland, C. M.; O'Reilly, J. M.; Sedita, J. S. *Macromolecules* 1992, 25, 3906.
- (27) Roland, C. M.; Ngai, K. L. *Macromolecules* 1992, 25, 5765.
- (28) Laughlin, W. T.; Uhlmann, D. R. *J. Chem. Phys.* 1972, 76, 2317.
- (29) Roland, C. M.; Santangelo, P. G.; Ngai, K. L.; Meier, G. *Macromolecules* 1993, 26, 6164.
- (30) Santangelo, P. G.; Roland, C. M.; Ngai, K. L. *Macromolecules*, in press.
- (31) A distinction must be made between dynamics at the molecular level and macroscopic properties such as dielectric constant or modulus. All segments relax at the same conformational transition rate. Molecular relaxation is heterogeneous on the time scale of  $\tau^*$ , however, because the intermolecular constraints inherent to the dense phase cause some of the attempted conformational transitions to fail. This results in statistical variations in the relaxation rate among segments. When averaged over all segments (as appropriate for macroscopic observables), homogeneous relaxation with a time-dependent relaxation rate is obtained.
- (32) Grest, G. S.; Cohen, M. H. *Adv. Chem. Phys.* 1981, 48, 455.
- (33) Ngai, K. L. In *Non-Debye Relaxation in Condensed Matter*; Ramakrishnan, T. V., Lakshmi, M. R., Eds.; World Scientific: Singapore, 1988; p 94.
- (34) Ngai, K. L.; Rendell, R. W.; Yee, A. F. *Macromolecules* 1988, 21, 3396.
- (35) Malhotra, B. D.; Pethrick, R. A. *Eur. Polym. J.* 1983, 18, 457; *Polym. Commun.* 1983, 24, 165.
- (36) Curro, J. J.; Roe, R.-J. *Polymer* 1984, 25, 1424.
- (37) Ng, D.; Aklonis, J. J. In *Relaxation in Complex Systems*; Ngai, K. L., Wright, G. B., Eds.; Government Printing Office: Washington, DC, 1985; p 53.
- (38) Rendell, R. W.; Ngai, K. L.; Fong, G. R.; Aklonis, J. J. *Macromolecules* 1987, 20, 1070.
- (39) Roland, C. M.; Ngai, K. L. *Macromolecules* 1991, 24, 2261.
- (40) Roland, C. M.; Santangelo, P. G.; Baram, Z.; Runt, J. *Macromolecules* in press.
- (41) Colmenero, J.; Alegria, A.; Ngai, K. L.; Roland, C. M. *Macromolecules* in press.
- (42) McCrum, N. G.; Read, B. E.; Williams, G. *Anelastic and Dielectric Effects in Polymer Solids*; Wiley: London, 1967.
- (43) Wetton, R. E.; Allen, G. *Polymer* 1966, 7, 331.
- (44) Sawada, K.; Ishida, Y. *Rep. Prog. Polym. Phys. Jpn.* 1974, 17, 437.
- (45) Boyd, R. H. *Polymer* 1985, 26, 323.
- (46) Ngai, K. L.; Roland, C. M. *Macromolecules* 1993, 26, 2688.
- (47) Nielsen, L. E. *Mechanical Properties of Polymers and Composites*; Marcel Dekker: New York, 1974; Vol. 1.
- (48) Flory, P. J. *J. Chem. Phys.* 1947, 15, 397.
- (49) Ngai, K. L.; Roland, C. M.; Yee, A. F. *Rubber Chem. Technol.* 1993, 66, 817.
- (50) Shi, J.-F.; Dickinson, L. C.; MacKnight, W. J.; Chien, J. C. W. *Macromolecules*, in press.
- (51) Mopsik, F. I. *Rev. Sci. Instrum.* 1984, 55, 79.
- (52) Coran, A. Y. In *Science and Technology of Rubber*; Ehrlich, F. R., Ed.; Academic Press: New York, 1978; Chapter 7.
- (53) Flory, P. J. *Polym. J.* 1985, 17, 1.
- (54) Ferry, J. D. *Viscoelastic Properties of Polymers*; Wiley: New York, 1980.
- (55) Glatz-Reichenback, J. K. W.; Sorriero, L.; Fitzgerald, J. J. *Macromolecules* 1994, 27, 1338.
- (56) Flory, P. J.; Erman, B. *J. Polym. Sci., Polym. Phys. Ed.* 1984, 22, 49.
- (57) Colmenero, J.; Alegria, A.; Santangelo, P. G.; Ngai, K. L.; Roland, C. M. *Macromolecules* 1994, 27, 407.